Design and realization of deep trench superjunction diode for 600V applications

Sylvain Noblecourt[1,2], **Josiane Tasselli**[1,3], **Frédéric Morancho**[1,2], **Karine Isoird**[1,2], **Patrick Austin**[1,2], **Pascal Dubreuil**[1,3], **Aurélie Lecestre**[1,3]

1. CNRS, LAAS, 7 av. du colonel Roche, 31400 Toulouse, France

2. Univ de Toulouse, UPS, LAAS, 31400 Toulouse, France

3. Univ de Toulouse, LAAS, 31400 Toulouse, France

ABSTRACT. *The purpose of this paper is to present the Deep Trench SuperJunction Diode (DT-SJDiode) optimization and realization with a 600V breakdown voltage. We present technological and geometrical parameters influences on the breakdown voltage with simulations performed with Sentaurus TCAD. Previous works allowed to validate some critical technological process steps and to create a technological process for 1200 V breakdown voltage applications. The main point here is to optimize those process steps (trench verticality, termination fulfilling...), which have an important influence on the electrical properties, in order to fabricate a 600 V breakdown voltage DT-SJDiode.*

RÉSUMÉ. *L'objectif de ce papier est de présenter l'optimisation et la réalisation d'une diode à superjonction et à tranchées profondes et de sa terminaison (DT-SJDiode) pouvant tenir des tensions de 600 V à l'état bloqué. Nous étudions l'influence des paramètres technologiques et géométriques sur la tenue en tension à partir de simulations effectuées sous Sentaurus TCAD. Des travaux précédents ont permis de valider certaines étapes technologiques et de dégager un procédé de fabrication pour des applications à 1200 V. Il s'agit ici d'optimiser ces différentes étapes qui influent sur les paramètres électriques (verticalité des tranchées, remplissage des tranchées de terminaison de jonction, etc.) pour des applications à 600 V.*

KEYWORDS: *superjunction diode, deep trench termination, BenzoCycloButene.*

MOTS-CLÉS : *diode à superjonction, terminaison à tranchées profondes, BenzoCycloButène.*

DOI:10.3166/EJEE.17.345-361 © Lavoisier 2014

1. Introduction

Today, up to 600 V-breakdown voltage, the main IGBT competitor is the MOSFET. Indeed, the MOSFET exhibits many interesting properties for power applications: high switching speed, high input impedance and thermal stability. However, in high voltage range (600 V and above), conventional MOSFETs are limited by their very high specific on-resistance and, therefore, their high on-state voltage drop, which induces more on-state losses, compared to bipolar devices. This specific on-state resistance is inversely proportional to the doping concentration of the drift region, which must be low enough to sustain the off-state voltage: to find the best trade-off between these two parameters (specific on-resistance/breakdown voltage) is one of the major challenges in this voltage range.

For this reason, several innovative unipolar structures have been proposed: the common idea is the structural modification of the drift region in order to overcome the theoretical limit of the 'specific on-resistance/breakdown voltage' trade-off of conventional unipolar power devices. The main concept is the well-known superjunction, which is implemented in power MOSFETs for years. It is based on the use of several sequences of "N-epitaxy then P-implantation" (or opposite) in order to realize the drift region, which is a vertical alternation of N and P columns. This technology was chosen in particular by Infineon for the realization of COOLMOS™ transistors (Lorenz *et al.,* 1999) and by STMicroelectronics for the realization of MDMESH™ devices (Sagio *et al*., 2000). However, the manufacturing cost of this technology can be very high because the process requires a significant number of masks. The breakdown voltage of these superjunction devices is also limited by the terminations (device peripheries) which are less effective when the drift region is strongly doped (which is the case and the interest of superjunction devices).

In this study, we propose new technological ways allowing the realization of deep trench superjunction devices (diodes and MOS transistors) with their appropriate termination (a deep trench termination) without using a multi-epitaxy process. Our objective is to set up a technology with a single epitaxial layer and the use of dielectric-filled, wide and deep trenches associated to boron doping on the trench sidewalls. Before realizing a superjunction MOSFET, we chosed to validate our technological choice by first fabricating a Deep Trench Superjunction Diode (DT-SJDiode) for 600V applications. The main challenges for the deep trench technology are the trenches verticality to ensure a perfect charge balance, the uniformity of the implantation on the trench sidewalls and the filling of the trenches with a dielectric.

The design and optimization of this DT-SJDiode are first performed by means of Sentaurus TCAD 2D-simulations. The objective is to determine the optimal physical and geometrical parameters allowing the achievement of the best "breakdown voltage/on-state resistance" trade-off. Then, we present the first technological results

focusing on the critical points of the developed technology, *i.e* control of the deep trenches verticality, P-doping on sidewalls and dielectric trench-filling.

2. Definitions and principles

2.1. Structure description

A cross-sectional view of the proposed DT-SJDiode is represented Figure 1. It is based on elementary cells allowing the implementation of the superjunction principle (Fujihira, 1997), *i.e.* an alternation of N and P regions in the volume. To ensure the maximal breakdown voltage, the superjunction is protected in periphery of the active zone by means of a guarding technique developed in the laboratory (Theolier *et al.*, 2009). We use a dielectric filled wide and deep trench with a field plate on top. The use of deep trenches allows to avoid a multi-epitaxy technology. The P^+ region is realized on the trench sidewalls from boron doping by Plasma-Immersion Ionic Implantation (PIII) (Nizou *et al.,* 2006). The dielectric is the BCB (Cyclotene 4026-46) (Dow Chemical Company, 2005) whose electrical parameters (critical field of 5.3 MV.cm^{-1} and dielectric constant of 2.65) allow to ensure the efficiency of the junction termination.

The parameters which are studied for the structure optimization are: the trench depth D_T, the implanted boron dose to obtain P^+ regions, the doping concentration of the N^- epitaxial zone, as well as the spacing W_N between two nearby central trenches. The N^- doping concentration is fixed at 3.10^{15} cm^{-3}: indeed, previous studies (Theolier, 2008) have shown that a higher concentration will increase the difficulty of the implantation step.

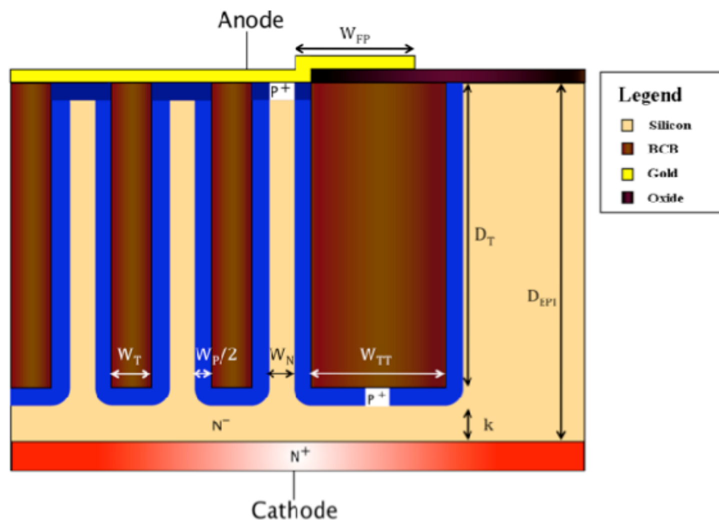

Figure 1. Schematic cross-section of the DT-SJDiode

2.2. Study of the "breakdown voltage/on-state resistance" trade-off

All the physical and geometrical parameters influence both breakdown voltage and on-state resistance. To obtain the best trade-off, we first have optimized the specific on-state resistance in order to study its impact on the breakdown voltage. To do so, we have simulated a single elementary cell, the central trench width W_T and the P^+ zone width W_P being respectively fixed to 6 µm and 1 µm.

The on-state resistance is mainly due to the drift resistance, which is the resistance of the N^- epitaxial layer. For a given doping concentration N_D, it can be assimilated to a simple bar of N type silicon of W_N-width and D_{EPI}–length or the trench depth D_T, assuming that: $D_{EPI} = D_T + k$, k being the distance between the bottom of the trenches and the N^+ substrate (k is kept constant in our study: k = 3 µm). Figure 2 shows the variations of the specific on-state resistance according to D_T for various values of W_N for a doping concentration N_D of 3.10^{15} cm^{-3}. A decrease in D_T or an increase in W_N leads naturally to a decrease in the specific on-state resistance.

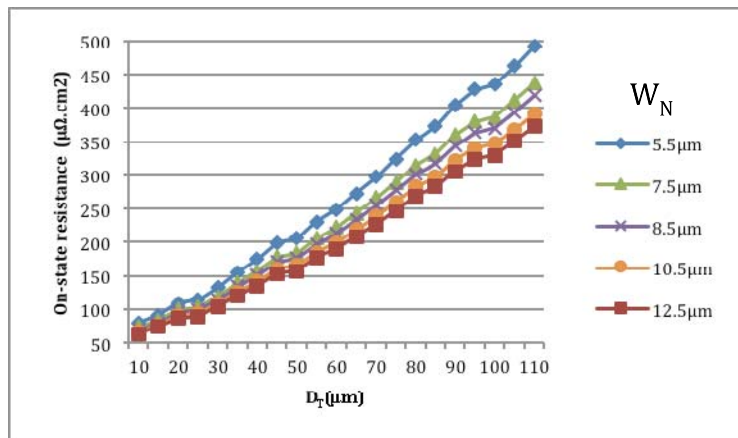

Figure 2. Simulated specific on-state resistance variations of an elementary cell as a function of trench depth D_T for various intercellular lengths W_N.

For an optimized superjunction, D_T is the key parameter allowing the adjustment of the desired breakdown voltage: the higher D_T, the higher the breakdown voltage. Figure 3 shows the variations of the breakdown voltage according to D_T.

The more the depth D_T increases and the more the depletion region increases thus increasing the electric field circulation and, consequently increasing the breakdown voltage. Unfortunately, the higher is D_T, the higher is the specific on-state resistance.

By correlating the data of Figure 2 and Figure 3, it is possible to determine the values of W_N and D_T which allow to obtain the best 'breakdown voltage/on-state resistance' trade-off. Figure 4 exhibits, for various desired breakdown voltages, the specific on-state resistance variations with the inter-trench width W_N. For instance, for a breakdown voltage of 600 V, it can be pointed out that, for W_N equals to 8.5, the specific on-state resistance presents a minimal value equal to 126 μΩ.cm^2.

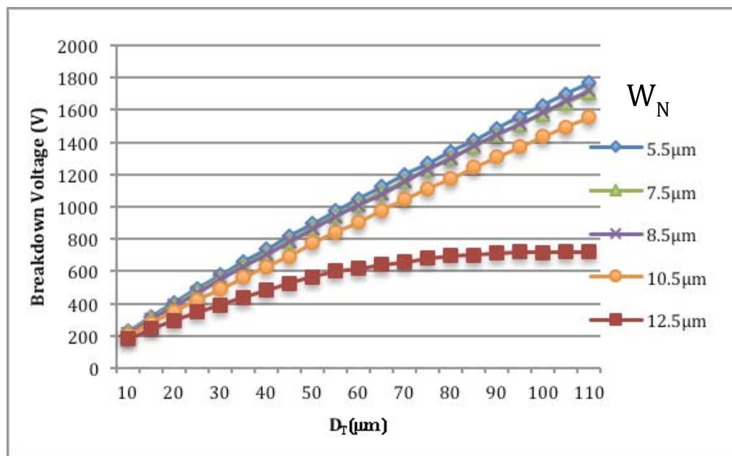

Figure 3. Simulated breakdown voltage variations according to the trench depth D_T for various values of W_N

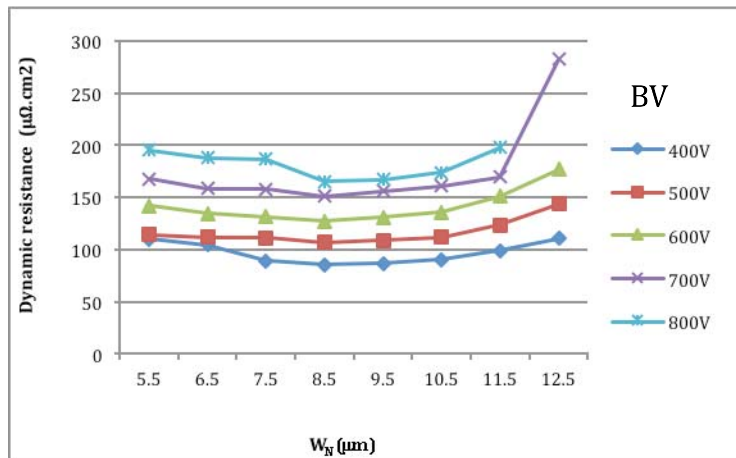

Figure 4. Simulated specific on-state resistance according to W_N for various values of breakdown voltage

The charge balance between N and P regions is important for the proper functioning of the superjunction and thus for the obtaining of an optimal breakdown voltage. Equation (1) reports this balance in the case of constant doping profiles. Couples (W_N ; N_D) and (W_P ; N_A) represent the widths and the doping concentration of N and P regions respectively:

$$W_N \,.\, N_D = W_P \,.\, N_A \tag{1}$$

An increase in W_N would naturally lead to a decrease in the specific on-state resistance because of the increase in the conduction section of the current. However, in this case, it would be necessary, as shown in equation (1), to act on the other parameters. The only constant parameter in our study is the doping concentration N_D of the N^- epitaxial layer: the value of 3.10^{15} cm^{-3} was chosen because this value theoretically allows a reasonable trade-off between electrical performance and technological constraints.

3. Optimization of diode parameters

3.1. Influence of the P^+ implantation dose

An increase in W_N implies an increase in the P^+ dose to keep the charge balance. However, the breakdown voltage becomes more sensitive to a charge unbalance compared to the optimal dose: then, P^+ implantation step becomes more critical because some percent of gap compared to the optimal dose makes fall drastically the breakdown voltage (see Figure 5).

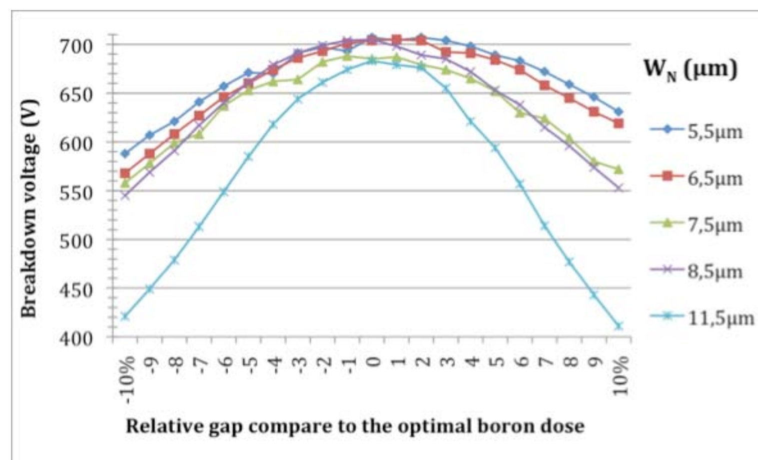

Figure 5. Simulated breakdown voltage variations as a function of the unbalanced boron dose in percent, referring to the optimal dose corresponding to the perfect charge balance, for various W_N values

It should be noted that, with our technology, this respect for the physical and geometrical parameters could be valid only if the trench sidewalls are perfectly vertical.

3.2. Optimization of the "W_N / D_T" couple

The trench depth D_T is the parameter allowing the determination of the optimal breakdown voltage. As already shown, the higher D_T, the higher the breakdown voltage. However, the specific on-state resistance R_{ON} will increase too. To overcome this specific on-state resistance increase, two options are possible: to increase the doping concentration N_D of the N^- epitaxial layer or to increase the width of the intercellular region W_N. As already mentioned, N_D was fixed to $3.10^{15}cm^{-3}$. Figure 3 shows the impact of the trench depth variations on the breakdown voltage for various values of W_N. From this figure, it can be deduced the minimal value of the trench depth allowing to obtain the minimal desired breakdown voltage of 600 V. Actually, the breakdown voltage variations are proportional to the trench depth D_T.

The obvious interest to increase W_N is to decrease the specific on-state resistance since W_N is the key parameter related to the conduction section of the device (the conduction section is the "silicon/insulator" ratio). However, the major consequence of this increase in W_N is the increase in the P^+ implantation dose necessary to ensure the good functioning of the superjunction. Indeed, it is necessary to act on the parameters that are concerned by the charge balance, *i.e.* the parameters of Equation (1). Given that the doping concentration of the epitaxial region N_D and the implantation depth are fixed, the only degree of freedom stays the implantation dose. Furthermore, beyond 12 µm ($W_N > 12$ µm), the drift region is not anymore able to deplete completely on the horizontal axis. It can be observed that, for $W_N > 12$ µm, the slope of the curve is different. The first reason is that it is necessary to have: $D_T >> W_N$ so that the principle of superjunction works. Indeed, the junction has to be laterally well depleted before depleting vertically to obtain a breakdown voltage, which is proportional to D_T and to the critical electrical field E_C. The second reason is due to the width W_P, which, even by increasing the P dose, will not be large enough. It would be theoretically possible to increase W_P but the PIII does not allow to implant deeply, thus we are limited by the width W_P.

3.3. Junction termination

For the junction termination, both interesting parameters are the width of the trench termination W_{TT} and the length of the field plate W_{FP}, the depth D_T being above all determined by the constraints of the elementary cell. They influence the breakdown voltage and the distribution and values of the electric field at breakdown.

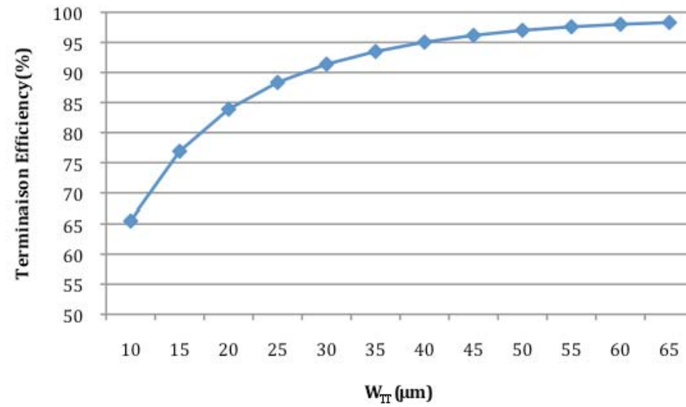

Figure 6. Simulated variations of the trench termination efficiency with W_{TT} for a 600 V breakdown voltage

The breakdown voltage of the termination depends above all on the parameter W_{TT}. Simulations of a plane junction using this trench termination were realized in order to determine the efficiency of this termination. Figure 6 shows that this efficiency reaches 95 % for a trench termination length of 40 µm.

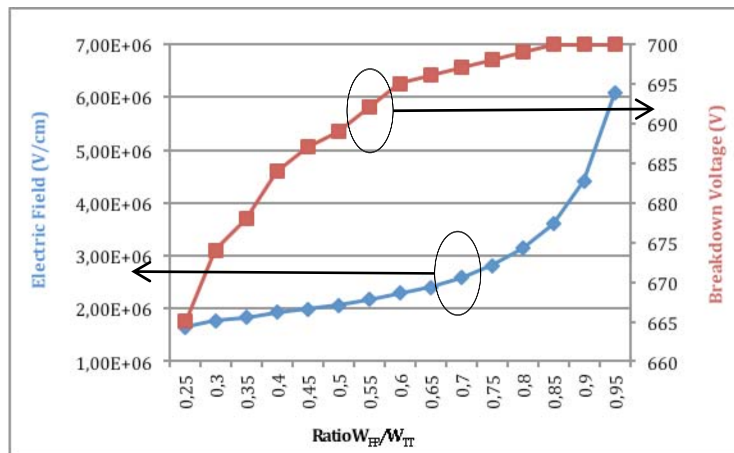

Figure 7. Breakdown voltage and maximal electrical field variations for various values of the 'W_{FP}/W_{TT}' ratio

As for the field plate length W_{FP}, more we increase it, better is the breakdown voltage. On the other hand, by increasing W_{FP}, the potential lines are tightened between the end of the field plate and the trench sidewalls and thus the electric field

reaches its critical value faster. Actually, this is not W_{FP} that is important but the "W_{FP}/W_{TT}" ratio. Figure 7 shows for instance that, for a ratio equal to 0.65, the electrical field at breakdown is about 2.4 x 10^6 $V.cm^{-1}$ and the breakdown voltage is close to 700 V. That means that there is a technological margin on the breakdown voltage but also on the electrical field that, as a reminder, does not have to exceed 3 $MVcm^{-1}$ at the risk of a premature breakdown in the air.

3.4. Results summary

According to the simulations previously presented, the optimal parameters of the DT-SJDiode were determined for a breakdown voltage of 600 V. Knowing that, at 600 V, the specific on-state resistance is almost similar for a W_N width between 8.5 µm and 11.5 µm (see Figure 4), we chose the 8.5 µm value because it allows to minimize the central cell size. According to Figure 5, the smallest possible value of P dose was chosen in order to limit breakdown voltage drops, which can occur with a bad precision of the implantation dose.

Table 1. Optimal parameters of the DT-SJDiode

Parameters	Symbols	Optimal values
N^- epitaxial region doping concentration	N_D	3 x 10^{15} cm^{-3}
Implanted P-dose	DoseP	1.44 x 10^{12} cm^{-2}
Distance between two central trenches	W_N	8.5 µm
P-region width	W_P	1 µm
Central trench width	W_T	6 µm
Trench depth	D_T	33 µm
Trench termination width	W_{TT}	40 µm
Field plate length	W_{FP}	26 µm
Breakdown voltage	BV	595 V
Specific on-state resistance	R_{ON}	126 $\mu\Omega.cm^2$

4. Experimental results

The optimization of the superjunction diode is related to some technological parameters, which could be critical to obtain the expected electrical performances, *i.e.* trench verticality, P implantation along the trench sidewalls and control of

dielectric filling. Indeed, to ensure a perfect charge balance between N and P regions, it is necessary to optimize the realization of the deep trenches to obtain etching sidewalls as vertical as possible with a lowest surface roughness. Another critical step is the filling of the deep trenches by a dielectric: breakdown voltage of the termination is dependent on its electric properties *i.e.* on the values of critical electric field (E_{Cd}) and permittivity (ε_{rd}). We present the different works we have performed in order to optimize these different technological steps.

4.1. Verticality of the trenches

The Deep Reactive Ion Etching (DRIE) is the more suitable technique to obtain a perfect verticality of trench sidewalls: it consists on an anisotropic etching based on an alternation of a Si etching step with SF_6 and a passivation step with C_4F_8. The main etching factors we can act on are the bias power, the pressure, the etching and passivation cycle times.

We have studied the influence of the passivation cycle time on the trench verticality. For an etching time fixed at 2 s, we have varied the passivation time from 1.5 s to 6 s for a gas flow rate fixed at 250 sccm. Between 1.5 s and 3 s, the etching profile is positive (the top width is wider than the bottom one) whereas beyond 3.5 s, the profile is negative. The most vertical profile is obtained for a passivation time of 3.5 s, as shown on Figure 8 for 5 µm wide and 53 µm deep trenches (etching time of 25 min): the difference between the width at the top and the bottom of the trench is 0.1 µm.

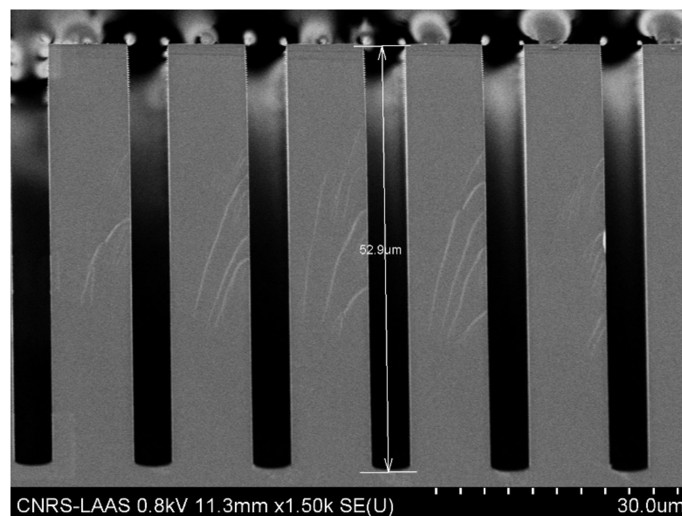

Figure 8. SEM pictures of a cross section for 25 min DRIE etching and a C_4F_8 passivation time of 3.5 s: the trenches are 5 µm wide and 53 µm deep

One of the characteristics of High Aspect Ratio (HAR) silicon etch using the Bosch process (Laermer *et al.*, 2003) is the scalloped shape of the sidewalls which is the consequence of the etching and passivation cycles alternation. The peak-to-valley distance can reach a 100 nm range (Figure 9a). One of the critical steps for the superjunction diode fabrication being the P implantation on the deep trench sidewall, it is necessary to reduce the scallop size. To do that, after trench etching, we perform a thermal oxidation: a 260 nm SiO_2 growth allows a 100 nm silicon material consumption. After a buffer HF wet etching, the oxide is eliminated and the peak-to-valley distance is reduced: it is lower than 50 nm as shown in Figure 9b.

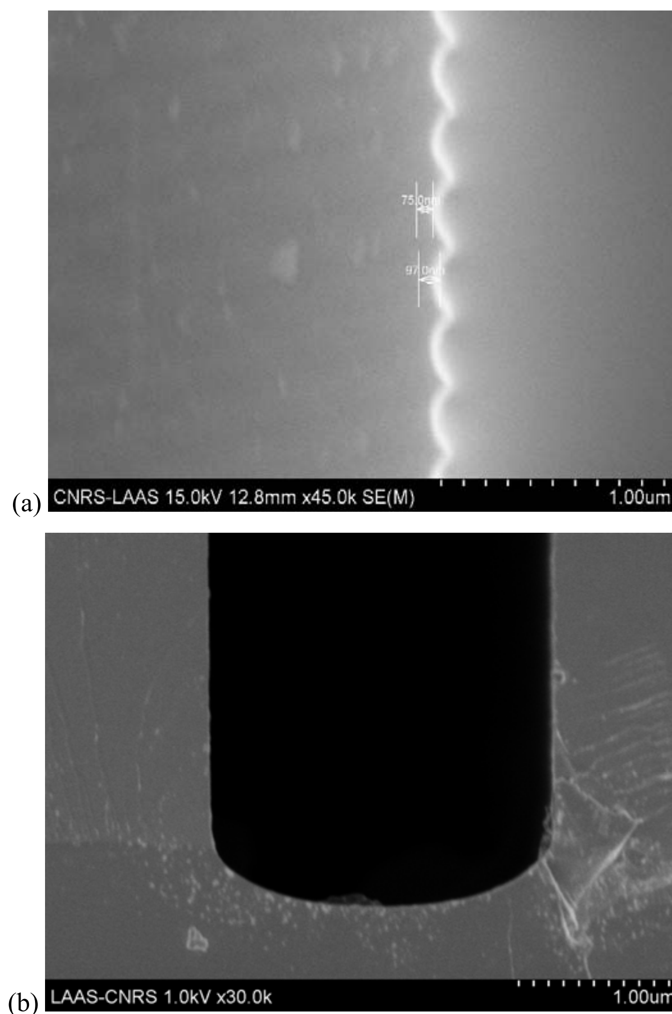

Figure 9. SEM picture of the scalloped shape of the trench sidewall after DRIE(a); after Si oxidation and buffer HF etching for scallop size reduction (b)

4.2. Reduction of the "ARDE" effect

The Aspect Ratio Dependent Etching effect (ARDE) is a limiting factor for the Bosch DRIE process: narrow trenches are etched slowly than large ones because of the reduction of ion bombardment and gas transport at the bottom of narrow and deep features (Chung, 2004). For our structure, the termination trenches are 40 µm wide whereas the trenches of the active central cells are 6 µm wide, inducing a deeper etching for the large ones. For example, for an etching time of 25 min and a 3.5 s C_4F_8 passivation time, the depth obtained for the central cells is 53 µm while it is around 95 µm for the termination trenches. From an electrical point of view, it does not influence on the breakdown voltage because the termination over crosses the epitaxial layer, fixed at 60 µm for a 600 V structure, and does not affect the charge balance. However if trenches are too deep, their dielectric filling becomes problematic.

In order to minimize the ARDE effect, we developed a technological process for the reduction of the etch rate difference between narrow and large trenches. A thermal silicon oxide mask is added only on top of the largest aperture before the photolithography resist patterning. The role of this oxide is to delay the etch beginning on the largest trenches.

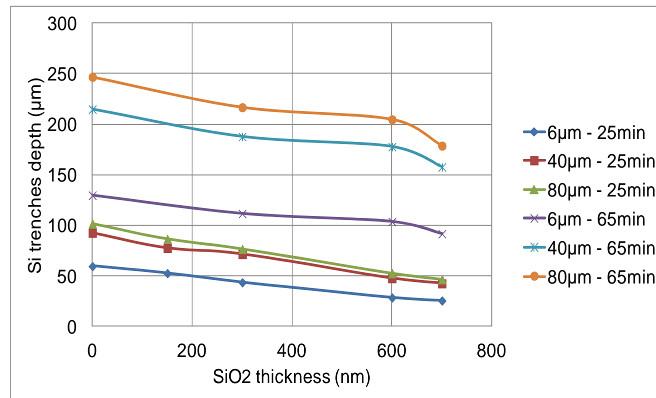

Figure 10. Silicon depth variations versus SiO_2 mask thickness for 25 min and 65 min etching times and different trench widths (6 µm, 40 µm, 80 µm)

The influence of the oxide thickness on etching depth for various trench widths is reported on Figure 10, for 25 min and 65 min etching times. For the latter, using a 300 nm thick oxide, the depth gap between 6 µm and 40 µm features is 70 µm, and the depth gap between 6 µm and 80 µm ones is 100 µm. In the case of a 1.6 µm thick oxide, the depth gap between 6 µm and 40 µm features is 5 µm, and the depth gap between 6 µm and 80 µm ones is 20 µm. These results are illustrated by the SEM pictures reported on Figure 11, for a 65 min DRIE etching time and a 3.5 s

passivation time, and for 300 nm and 1.6 µm oxides (Figure 11a and 11b respectively).

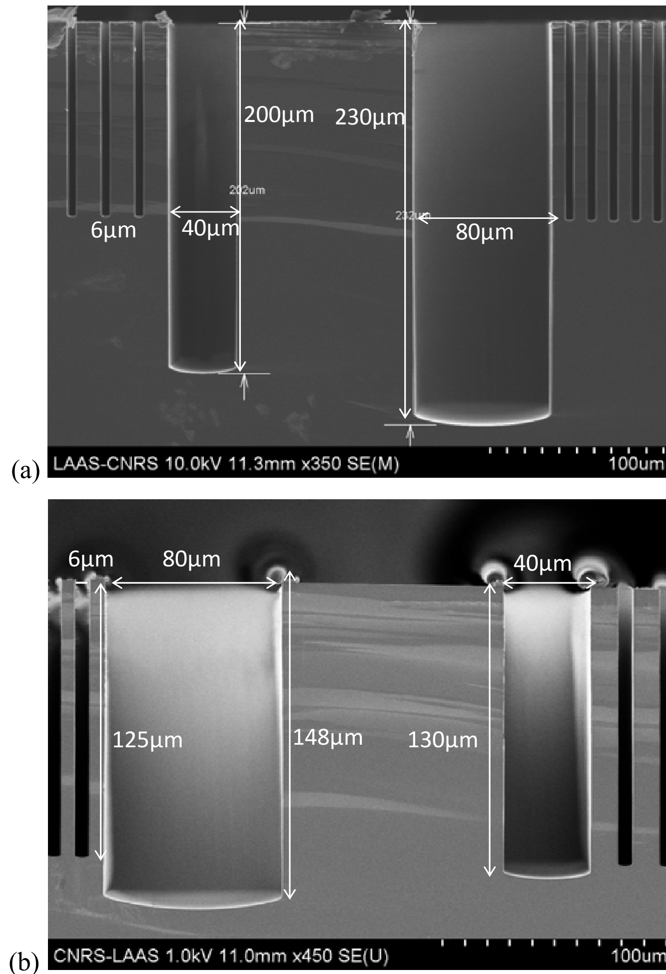

Figure 11. SEM picture of trenches with high aspect ratio (HAR >28) for an etching time of 65 min through an oxide layer of 300 nm thick (a) and 1.6 µm thick (b)

4.3. Dielectric filling of the trenches

Among the available dielectric materials for trench filling, the Cyclobutene 4026-46 (BCB) is a good candidate (E_{Cd} = 5.3 MV/cm and ε_{rd} = 2.65). Previous works allowed to validate this technological step for 1200 V breakdown voltage diodes (Theolier *et al.,* 2009). However, to achieve a complete deep termination

trench filling, it was necessary to perform two successive BCB spin-coatings, associated to two chemical-mechanical polishing steps to remove the excess of dielectric on top of the structure. We have developed a new technological process in order to rend the process more simple with only one deposition of BCB.

We have first worked on the etching step to obtain a same depth for trenches with different widths as shown in paragraph 4.2, thus lowering the necessary BCB quantity. We also optimized the BCB coating parameters: the results are given in Table 2. Because of the high viscosity of BCB material, a small spinner rotation speed (100 rpm) associated to a rest stage favors narrower trenches filling while the spreading step favor the excess material escape. BCB is then soft baked on a hot plate at 90°C for 5 min to remove the solvent and to stabilize the film, followed by hard curing at 250°C for 60 min under N_2 ambient.

Table 2. BCB spin-coating parameters

Spin-coating steps	Time	Rotation Speed	Acceleration
BCB dispensing	60 s	100 rpm	100 rpm^2
BCB spreading	30 s	200 rpm	200 rpm^2
Rest	10 min		
BCB spreading	10 s	1000 rpm	1000 rpm^2
Rest	10 min		

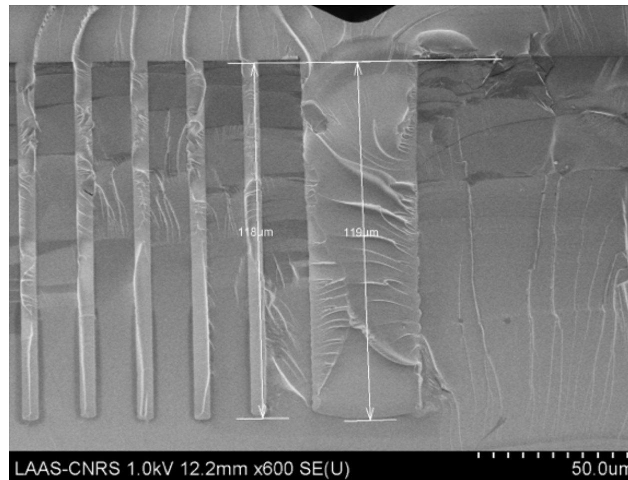

Figure 12. Cross-sectional SEM view of trenches filled with one BCB spin-coating

Figure 12 shows a SEM cross-sectional view of 6 µm and 40 µm wide and 120 µm deep trenches successfully filled with only one BCB spin-coating. Resulting BCB thickness on top of the wafer is 40 µm.

We have investigated the capability to remove the BCB excess by reactive ion etching instead of chemical-mechanical polishing: the challenge is the high thickness to be etched, *i.e.* tenth of microns. We first studied BCB etching with a photoresist mask using both fluorine and oxygen such as SF_60_2 gas mixture (Chen *et al.,* 2010): the fluorine removes the silicon in BCB and the oxygen reacts with the carbon and organic content. We analyzed the influence of the plasma etching parameters, *i.e.* RF power, chamber pressure, gas composition ratio, on the etching rate, BCB selectivity to photoresist and anisotropy. First results are shown in Figure 13 for a 40 µm BCB layer and 14 µm AZ photoresist: after 10 min etch (Figure 13a), a same 7.5 µm thickness of resist and BCB has been etched; after 20 min etch (Figure 13b) there is no more resist and half of BCB is etched, *i.e.* 20 µm. This indicates that BCB and photoresist have the same etch rate, around 0.75 $\mu m.min^{-1}$. We obtained residue-free etching for the applied plasma conditions.

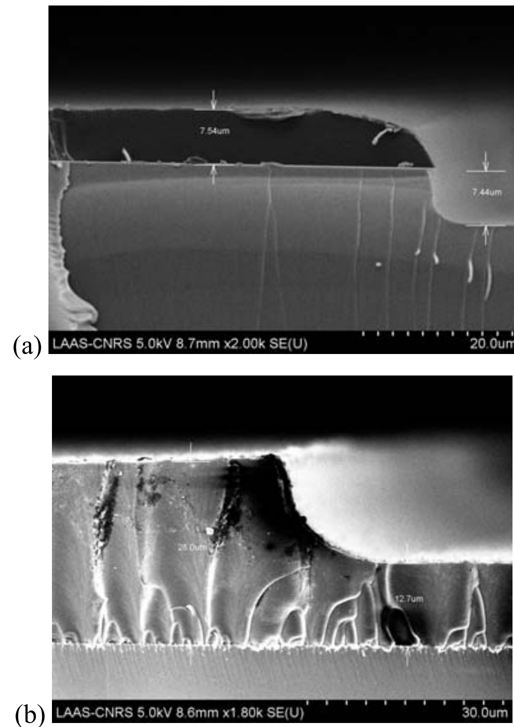

Figure 13. Cross-sectional SEM view of BCB etch after 10 min (a) and 20 min (b) with 14 µm photoresist mask, SF6 (15 sccm)/O2 (200 sccm) plasma, 40 W RF power, and 0.2 mT chamber pressure

However BCB etching is not anisotropic: this is due to the plasma conditions to be optimized but also to the slope observed in the resist profile after the soft-bake step (Figure 13a). The resist profile is transferred into BCB layer during etch. So future works will concern, in particular, the optimization of the etch mask: we will investigate either a thicker resist layer by controlling its soft-bake or a metal hard mask such aluminum thin film.

5. Conclusion

New technological ways allowing the realization of deep trench superjunction devices (diodes or MOS transistors) with a deep trench termination are proposed. We developed a technology based on a single N^- epitaxial layer and the use of BCB filled, wide and deep trenches associated to boron doping on the trench sidewalls. Previous works have demonstrated the feasibility of such junction termination and have led to the fabrication of a 1200 V Deep Trench Termination Diode. We chose to validate our technological choice by fabricating a Deep Trench Superjunction Diode (DT-SJDiode) for 600 V applications.

By means of Sentaurus TCAD 2D-simulations, we have first determined the optimal physical and geometrical parameters leading to a best 'breakdown voltage/on-state resistance' trade-off. For example, for a N^- epitaxial region doping concentration of 3×10^{15} cm^{-3}, a distance between two central trenches of 8.5 µm and a trench termination width of 40 µm, the breakdown voltage is 595 V and the specific on-state resistance is 126 $\mu\Omega.cm^2$.

We presented technological results focusing on the control of deep trench verticality by Deep Reactive Ion Etching technique, and the trench filling with dielectric. We have studied the influence of SF_6 etch and C_4F_8 passivation times on resulting trench verticality: the best anisotropy for 6 µm wide central trenches and 40 µm wide termination trenches is obtained for the couple SF_6 (2 s)/ C_4F_8 (3.5 s). A thermal oxidation after the etch step allows to reduce the size of the scallops that appear on the trenches sidewalls due to the Bosch process.

Finally we have successfully filled deep and wide trenches by optimizing the BCB spin-coating parameters: dispensing rotation speed down to 100 rpm, implementation of two 10 min rest steps improve BCB spreading and its flowing along the trenches. The BCB excess removing by reactive ion etching is under study: first encouraging results give an etch rate of 0.75 $\mu m.min^{-1}$ with a $SF_6/0_2$ gas mixture.

A complete fabrication process, integrating the above technological steps associated to the boron implantation on the trenches sidewalls, is in progress for the realization of 600 V DT-SJ Diodes and DT-SJMOSFETs.

Acknowledgements

For this work, the authors acknowledge the support of the French RENATECH Network and the French Agence Nationale de la Recherche (ANR) under reference ANR-2011-B509-033 ("SUPERSWITCH" project)

Bibliography

Chen Q. (2010). Characterization of reactive ion etching of benzocyclobutene in SF6/02 plasmas. *Microelectronic Engineering*, 87, p. 1945-1950

Chung C-K. (2004). Geometrical pattern effect on silicon deep etching by an inductively coupled plasma system. *Journal of Micromechanics and Microengineering*, 14, p. 656-662

Dow Chemical Company Processing for CYCLOTENE 4000 Series Photo BCB Resins, Février 2005.

Fujihira T. (1997). Theory of semiconductor superjunctions devices. *Japanese Journal of Applied Physics*, vol. 36, p. 6254-6262.

Learmer F. (2003*). Method of anisotropic etching of silicon*. Patent n° 6,531,068 B2.

Lorenz L. (1999). COOLMOS™ – a new milestone in high voltage power MOSFET. ISPSD, p. 3-10.

Nizou S. (2006). Deep Trench doping by plasma immersion ion implantation in silicon. *16th International conference on Ion Implantation Technology*, p. 229-232.

Sagio M. (2000). MDMESH™: innovative technology for high voltage power MOSFETs. ISPSD, p. 65-68.

Théolier L. (2009). A new junction termination technique: the Deep Trench Termination (DT2). ISPSD, p. 176-179.

Théolier L. (2009). A New Junction Termination Using a Deep Trench Filled With BenzoCycloButene. *IEEE Electron Device Letters*, vol. 30, n° 6, p. 687-689.

Théolier L. (2008). *Conception de transistors MOS haute tension (1200 V) pour l'électronique de puissance*. Thesis.

Received: 3 February 2015
Accepted: 27 October 2015